

Soot Track Formation by Shock Wave Propagation

K. Inaba¹, M. Yamamoto², J.E. Shepherd³ and A. Matsuo⁴

Summary

The purpose of this research is to explore an explanation of detonation soot track formation, comparing with previous hypothesis of formation mechanism. Focusing on the role of shear stress in transporting soot along the surface, we investigated the non-reactive Mach reflections numerically with three-dimensional compressible Navier-Stokes simulations. Numerical results are compared with a two-dimensional detonation simulation and used to investigate the effect of shear stress spatial and temporal variations on soot redistributions. The motions of soot due to surface shear stress are numerically examined with treating soot as particles and fluid parcel.

Introduction

The soot track method has been widely used as an indication of detonation propagation and a semi-quantitative tool for measuring the cell size and classifying the regularity of the cellular structure (Fickette and Davis [1]). Although it is obvious that the soot tracks are related to frontal shock waves, triple-point trajectories measured by PLIF of the OH radical distribution near the soot foil do not accord with the soot tracks in the experiment of Pintgen and Shepherd [2]. Hypothesis on the mechanism has included pushing the soot with pressure gradients, "scrubbing" the soot off by vortices [3], and combustion of the soot in hot oxidizing atmospheres [4]. However, the precise physical mechanism that creates the soot tracks has never been clearly demonstrated. The goal of the present study is to explore an explanation that is based on the classical fluid mechanics of near-wall flow in a viscous gas.

We proposed that the soot tracks depend largely on variations in the direction and magnitude of the shear stress created by the boundary layer over the soot foil. Our proposal is motivated by three key observations: 1) soot tracks can be formed in Mach reflection of a non-reactive shock [5], 2) pattern formation in oil flow visualization can be completely explained in terms of surface shear stress [6], and 3) the process of Mach reflection in a non-reactive gas contains all the essential features of the shock configurations in detonation fronts. We will perform a preliminary simulation of a 2-D detonation to detect the flow characteristics, and a simulation of a Mach reflection to estimate the shear stress and pressure distribution. In this paper, simple models of soot motions will be constructed and examined to interpret

¹Research Associate, Tokyo University of Science, Japan

²Professor, Tokyo University of Science, Japan

³Professor, California Institute of Technology, USA

⁴Associate Professor, Keio University, Japan

the influences of shear stress, treating the soot layer as clumps of fine particles and as incompressible fluid.

Numerical Setup

A flow field for a detonation propagating is a stoichiometric $2\text{H}_2+\text{O}_2+3.76\text{N}_2$ mixture at the initial static pressure 20 kPa and static temperature 298.15 K. The C-J Mach number M_{CJ} and the half-reaction length $L_{1/2}$ are 4.92 and 452 μm , respectively. The 2-D Euler equations for a chemically reacting gas mixture are adopted as the governing equations. The 9-species, 19-reaction mechanism [7] is used for hydrogen-air combustion. Yee's non-MUSCL-type TVD upwind explicit scheme [8] is employed for the inviscid term in the equations. The computation is performed with a constant grid resolution of 50 grid points/ $L_{1/2}$ along the x -axis. The channel width where a detonation propagates is 3.6 mm ($=8.0 L_{1/2}$).

A simulation of a Mach reflection over a wedge is carried out at the similar condition of the frontal shock configuration in the detonation wave. The flow behind the shock wave is investigated by numerically simulating the 3-D compressible Navier-Stokes equations. Initial conditions are followings; 298.15 K at the static temperature, Mach 4.92, an apex angle of the wedge $\theta_w = 33.1$ degree, unit Reynolds number $\text{Re} = 1.8 \times 10^7$ m. As shown in Fig. 1, a stretched grid system is used and the number of grid points is $151 \times 51 \times 101$ ($5.3 \times 0.7 \times 3.6$ mm). We adopt a shock-fixed coordinate system; the bottom $x - z$ plane (a non-slip and isothermal boundary condition) corresponds to a soot foil and is moving at the same speed as the shock. The modeling of soot motion is carried out with two aspects; the first is that the soot is treated as a continuum; the second is that the soot is regarded as aggregate of solid particles.

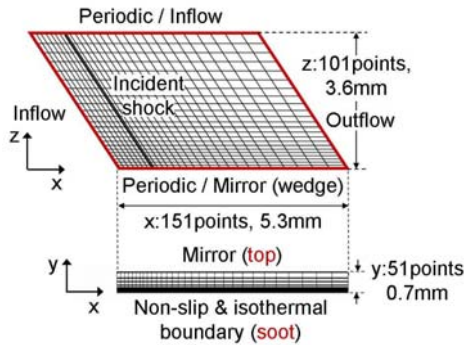


Figure 2: Instantaneous pressure contours of the detonation front (p_1 , post-incident shock pressure; p_3 , post-

Figure 1: Computational domain and reflected shock pressure).
boundary conditions.

Fluid model

Assuming that the soot is approximated as an incompressible fluid, the soot thickness h can be expressed the following conservation equation [6];

$$\frac{\partial h}{\partial t} + \frac{\partial (hu)}{\partial x} + \frac{\partial (hw)}{\partial z} = 0, \quad u = \frac{\tau_{yx}h}{2\mu_s}, \quad w = \frac{\tau_{yz}h}{2\mu_s} \quad (1)$$

where u , w , τ_{yx} , τ_{yz} are the velocity components and the shear stresses arising from the gaseous boundary layer in x and z directions, respectively, and μ_s is viscosity of the soot layer. The governing equations (1) are discretized with MacCormack scheme [9] in the 2-D computational domain that has the same cross-sectional area of 3-D grid for air. Shear stresses of air drive soot, though soot-thickness distributions do not affect air flow; hence, one-way coupling is assumed.

Particle model

The discrete particle approach is utilized for numerical simulations. The particle is assumed to consist of spherical particles which distribute in the computational $x-z$ plane. The governing equations of soot particles become followings;

$$\frac{\partial \mathbf{I}_i}{\partial t} = \mathbf{F}_i \quad \mathbf{I}_i = \begin{bmatrix} x_i \\ z_i \\ u_i \\ w_i \end{bmatrix} \quad \mathbf{F}_i = \begin{bmatrix} u_i \\ w_i \\ (f_x/m_p)_i \\ (f_z/m_p)_i \end{bmatrix} \quad (2)$$

where $f_x = \pi \overline{\tau_{yx}} r_p^2$, $f_z = \pi \overline{\tau_{yz}} r_p^2$ are tractive forces for x , z -components, $m_p = 4/3\pi\rho_s r_p^3$ and r_p are mass and radius of a soot particle, respectively, and ρ_s ($=1200 \text{ kg/m}^3$) is soot density. The governing equations (2) are solved by the fourth-order Runge-Kutta method. Initially, 64 particles are arranged in each computational cell.

Results and Discussion

Preliminary simulation of 2-D Detonation

Frontal properties are examined to determine parameters for the Mach reflection simulation reproducing the shock configuration of the detonation wave. The parameters for Mach reflections are transverse wave strength, defined by the pressure jump across the reflected shock wave, and entrance angles of triple-point track. Figure 2 indicates the instantaneous pressure contours of the detonation front. Frontal shock configuration is a double-Mach reflection (DMR). The transverse wave strength S ($= p_3/p_1 - 1$) is approximately 0.9, where p_1 and p_3 are the post-incident and the post-reflected shock pressures, respectively. Detonation history presented by the maximum pressure contours is depicted in Fig. 3. The entrance angle of the triple-point track α is about 40 degree, and is quite proper to the present transverse wave strength ($S = 0.9$) [1].

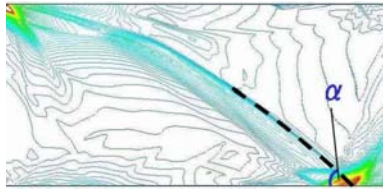


Figure 3: Maximum pressure history produced by the detonation propagation (α , the entrance angle of the triple point track).

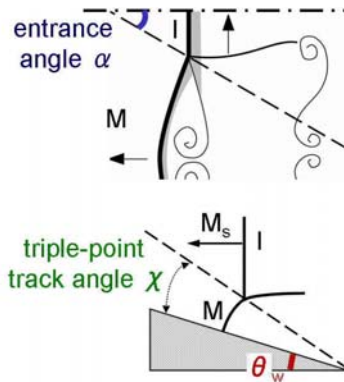


Figure 4: Analogy between the detonation front and the Mach reflection over a wedge.

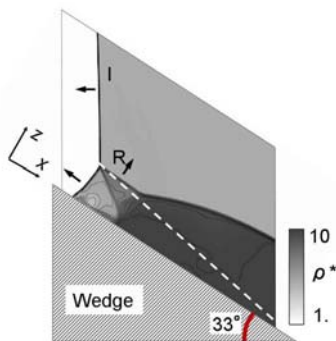


Figure 5: Instantaneous density distribution on the opposite side of the soot foil.

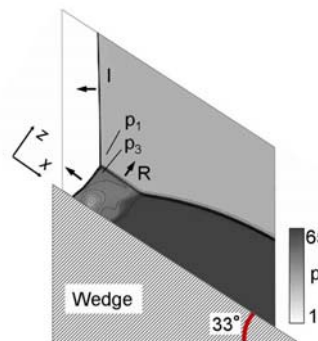


Figure 6: Instantaneous pressure distribution on the opposite side of the soot foil.

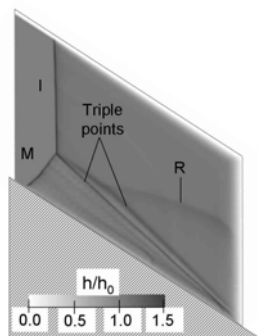


Figure 7: Soot thickness distribution by fluid model.

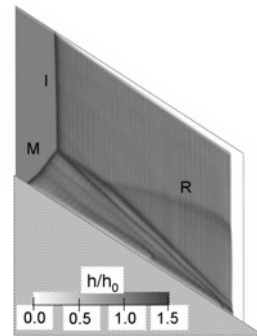


Figure 8: Soot thickness distribution by particle model.

3-D Simulation of Mach reflection (Air, non-reactive gas)

Figure 4 illustrates the correlation between a detonation front and a Mach reflection over a wedge. The Mach reflection consists of the Mach stem and the incident shock wave as well as the detonation front. The summation of the track angle of a triple-point χ derived from the three-shock theory and an apex angle of the wedge θ_w equal the entrance angle α ($= \chi + \theta_w$). According to the relation, θ_w is determined to 33.1 degree.

Figures 5 and 6 show the instantaneous flow features of the density and pressure distributions on the opposite side of the soot foil, respectively. This is because the flow features inside the boundary layers are obscured by the boundary layer induced by the shock waves. In the density distribution (Fig. 5), DMR appears, and the track angle of the triple point χ is about 9.4 degree. The entrance angle α ($= 42.1$ degree) is in a good agreement with that of the detonation case. Pressure distribution as shown in Fig. 6 demonstrates the transverse wave strength equals to 0.8, which is close to 0.9 in the detonation front.

Simulations of soot redistribution

Simulations of soot thickness are performed, using shear stress histories of gas phase. Figure 7 shows the soot thickness h normalized by the initial soot thickness h_0 with the fluid model in the form of gray-scale distribution. The shock front propagates from right to left. Soot is piled up around a triple-point track due to breaks on a frontal shock and a reflected shock. While one soot track is formed on the Mach stem side in SMR in our previous results [10], it is also formed on the incident shock side in DMR in the present study. In this model, parameters are initial soot thickness h_0 ($= 1.7$ mm) and soot viscosity. The soot viscosity is not well known and is approximated with the property of glycerin $\mu_{glycerin}$ ($= 14.9 \times 10^{-4}$ Pa s) at 298.15 K. As the initial soot thickness decreases with μ_s , variation of soot thickness becomes flattened, and at last most of the soot just remains on the wall. Even if arbitrary viscosity coefficient is chosen (e.g. $\mu_{air} = 18.2 \times 10^{-6}$ Pa s), the same feature of soot tracks can be obtained with the appropriate initial thickness ($h_0 = 2.0$ μ m for air).

With the particle model, a similar result to the fluid model is obtained as shown in Fig. 8. Parameters in the particle model are initial soot thickness h_0 ($= 20$ μ m) and particle radius r_p ($= 0.27$ nm). In this model, initial soot thickness is not important for the soot track, but the particle radius dominates the magnitude of soot thickness variations. Parameters are chosen by the same criterion as the fluid model and thus the computational particle radius of 0.27 nm becomes much smaller than that of typical soot particle radius. Although drag force and skin friction do not affect the present results, further force assessment might be necessary, such as pressure gradients. Similar soot distributions are obtained by fluid and particle models

by choosing appropriate parameters.

Summary

Soot track formation was numerically investigated, assuming that the soot tracks were due to variations in the direction and magnitude of the shear stress created by the boundary layer over the soot foil. Two-dimensional $2\text{H}_2+\text{O}_2+2\text{N}_2$ detonation was simulated to examine frontal properties and determine the parameters for Mach reflection simulation to reproduce the same shock configuration as detonation. In non-reactive air, double Mach reflection appeared by using the determined parameters, and shear stress vectors suddenly changed their directions across the triple point and a reflected shock. Using gaseous shear stress, similar soot distributions are obtained by fluid and particle models by choosing appropriate parameters. Soot is piled up around a triple-point track due to breaks on the frontal shock and the reflected shock. While soot track is formed on the Mach stem side in single Mach reflection, it is also formed on the incident shock side in double Mach reflection.

References

1. Fickett, W. and Davis, W. C., "Detonation," *University of California Press*, Berkeley, 1979, Chap. 7.
2. Pintgen F. and Shepherd, J. E., *Proc. 19th ICDERS*, Hakone, Japan, 2003.
3. Krehl, P. and Geest, van del M., *Shock Waves*, 1, 1991, 3-15.
4. Terao, K. and Azumatei, T., *Jpn. J. Appl. Phys.*, 28, 1989, 723-728.
5. Lam, A. K. W., Austin, J. M., Pintgen, F., Wintenberger, E., Shepherd, J. E., Inaba, K., Matsuo, A., *Proc. 19th ICDERS*, Hakone, Japan, 2003.
6. Tanner, L. H. and Blows, L. G., *J. Phys. E, Scientific Instruments*, 9, 1976, 194-202.
7. Wilson, G. J., and MacCormack, R. W., AIAA-90-2307, 1990.
8. Yee, H. C., *NASA TM 89464*, 1987.
9. MacCormack, R. W., *AIAA Paper 69-354*, 1969.
10. Inaba, K., Matsuo, A., Shepherd, J. E., *Proc. 20th ICDERS*, Montreal, Canada, 2005.